

Carbon–Carbon Bond Formation Using Yttrium(III) and the Lanthanide Elements

Michael D. Fryzuk,* Laleh Jafarpour, Francesca M. Kerton, Jason B. Love, Brian O. Patrick,[†] and Steven J. Rettig[†]

Department of Chemistry, University of British Columbia,
2036 Main Mall, Vancouver, B.C., Canada V6T 1Z1

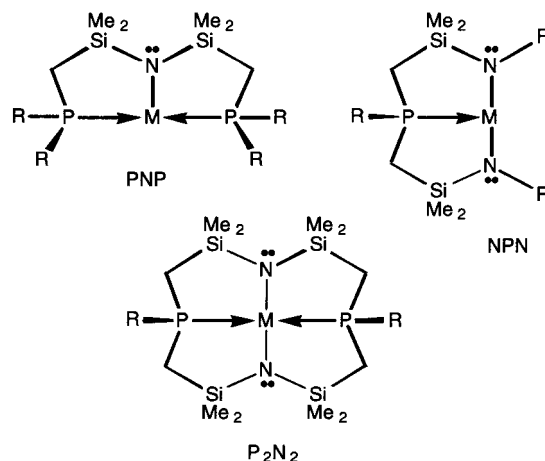
Received August 30, 2000

The synthesis and characterization of a series of yttrium and lanthanide complexes that incorporate the macrocyclic bis(amidophosphine) ligand $\text{PhP}(\text{CH}_2\text{SiMe}_2\text{NSiMe}_2\text{CH}_2)_2\text{PPh}$, $[\text{P}_2\text{N}_2]$, are described. The starting materials, $\{[\text{P}_2\text{N}_2]\text{M}\}_2(\mu\text{-Cl})_2$, ($\text{M} = \text{Y}, \text{Sm}, \text{Ho}, \text{Yb}, \text{Lu}$), are prepared by the reaction of *syn*- $\text{Li}_2(\text{dioxane})[\text{P}_2\text{N}_2]$ with $\text{MCl}_3(\text{THF})_3$ in toluene. The reactivity of these complexes toward PhLi and other arylating agents is dependent on the size of the M^{3+} ion. $\text{M} = \text{Y}$ and Ho undergo C–C bond formation reactions to give biphenyldiide compounds $\{[\text{P}_2\text{N}_2]\text{M}\}_2\{\mu\text{-}\eta^6\text{:}\eta^6\text{-(C}_6\text{H}_5)_2\}$ and $\{[\text{P}_2\text{N}_2]\text{Y}\}_2\{\mu\text{-}\eta^6\text{:}\eta^6\text{-(C}_6\text{H}_4\text{-}i\text{p-Ph})_2\}$. These have been structurally characterized and show the biphenyl dianion bridging two $[\text{P}_2\text{N}_2]\text{M}$ fragments. These $[\text{P}_2\text{N}_2]\text{M}$ fragments migrate over the bridging ligand's π -surface on the NMR time scale. $\text{M} = \text{Yb}$ yields the paramagnetic monophenyl derivative $[\text{P}_2\text{N}_2]\text{Yb}(\text{C}_6\text{H}_5)$, where the Yb center is coordinatively unsaturated and resides in a distorted square-pyramidal environment. $\text{M} = \text{Lu}$ results in a mixture of “ate” complexes of the formulation “ $[\text{P}_2\text{N}_2]\text{LuPh}\cdot\text{LiCl}$ ”, as evidenced by ^7Li NMR. However, the biphenyl product $\{[\text{P}_2\text{N}_2]\text{Lu}\}_2\{\mu\text{-}\eta^6\text{:}\eta^6\text{-(C}_6\text{H}_5)_2\}$ can be synthesized via a reductive route. The presence of THF was found to be deleterious to the coupling reaction; in this case, the THF adduct $[\text{P}_2\text{N}_2]\text{Y}(\text{C}_6\text{H}_4\text{-}i\text{p-Me})\text{(THF)}$ was isolated and structurally characterized. The mechanism for the C–C bond formation reaction is described based on the isolation of these yttrium and lanthanide complexes.

Introduction

Because of the recent prominence of d^0 metal complexes as potential catalysts in a variety of processes,^{1–6} exploratory work on the discovery of new complexes of the early transition elements and the lanthanides has intensified. One particularly popular avenue has been to move away from the traditional cyclopentadienyl-type ligand systems to other donor sets.^{7–11} Our own work has concentrated on developing mixed donor chelating and macrocyclic ligands with amido and phosphine donors in varying ratios.^{12–19} This has led to the design

Chart 1



[†] Professional Officers: UBC X-ray Structural Laboratory: S.J.R. deceased October 27, 1998.

- (1) Bochmann, M. *J. Chem. Soc., Dalton Trans.* **1996**, 255.
- (2) Grimmond, B. J.; Corey, J. Y. *Organometallics* **1999**, *18*, 2223.
- (3) Gountchev, T. I.; Tilley, T. D. *Organometallics* **1999**, *18*, 5661.
- (4) Tian, S.; Arredondo, V. M.; Stern, C. L.; Marks, T. J. *Organometallics* **1999**, *18*, 2568.
- (5) Douglass, M. R.; Marks, T. J. *J. Am. Chem. Soc.* **2000**, *122*, 1824.
- (6) Alt, H. G.; Koppl, A. *Chem. Rev.* **2000**, *100*, 1205.
- (7) Edelmann, F. T. *Angew. Chem., Int. Ed. Engl.* **1995**, *34*, 2466.
- (8) Evans, W. J. *New J. Chem.* **1995**, *19*, 525.
- (9) Britovsek, G. J. P.; Gibson, V. C.; Wass, D. F. *Angew. Chem., Int. Ed.* **1999**, *38*, 428.
- (10) Gade, L. H. *Chem. Commun.* **2000**, 173.
- (11) Kempe, R. *Angew. Chem., Int. Ed.* **2000**, *39*, 468.
- (12) Cohen, J. D.; Fryzuk, M. D.; Loeher, T. M.; Mylvaganam, M.; Rettig, S. J. *Inorg. Chem.* **1998**, *37*, 112.
- (13) Fryzuk, M. D.; Giesbrecht, G.; Rettig, S. J. *Organometallics* **1996**, *15*, 3329.
- (14) Fryzuk, M. D.; Love, J. B.; Rettig, S. J.; Young, V. G. *Science* **1997**, *275*, 1445.
- (15) Fryzuk, M. D.; Love, J. B.; Rettig, S. J. *Organometallics* **1998**, *17*, 846.
- (16) Fryzuk, M. D.; Johnson, S. A.; Rettig, S. J. *J. Am. Chem. Soc.* **1998**, *120*, 11024.

of three classes of ancillary ligands (PNP, NPN, and P_2N_2 , Chart 1) for which electronic and steric effects, as well as overall charge, can be varied with considerable flexibility. As part of our efforts at exploring the organometallic chemistry of the early transition elements and the lanthanides with the above ligand sets, we were intrigued by the discovery of some deeply

(17) Fryzuk, M. D.; Leznoff, D. B.; Thompson, R. C.; Rettig, S. J. *J. Am. Chem. Soc.* **1998**, *120*, 10126.

(18) Fryzuk, M. D.; Leznoff, D. B.; Ma, E. S. F.; Rettig, S. J.; Young, V. G. *Organometallics* **1998**, *17*, 2313.

(19) Fryzuk, M. D.; Johnson, S. A.; Rettig, S. J. *Organometallics* **1999**, *18*, 4059.

Table 1. Crystallographic Data

	1a	1e	3c	5	6	8
formula	C ₄₈ H ₈₄ Cl ₂ N ₄ P ₄ Si ₈ Y ₂	C ₄₈ H ₈₄ Cl ₂ N ₄ P ₄ Si ₈ Lu ₂	C ₆₀ H ₉₄ N ₄ P ₄ Si ₈ Ho ₂	C ₇₉ H ₁₁₀ N ₄ P ₄ Si ₈ Y ₂	C ₃₇ H ₆₂ N ₂ O _{1.50} P ₂ Si ₄ Y	C ₃₀ H ₄₇ N ₂ P ₂ Si ₄ Yb
fw	1314.52	1486.64	1549.87	1642.16	822.10	783.04
color, habit	colorless, irregular	colorless, irregular	black, block	blue, needle	clear, needle	orange, block
cryst size, mm	0.20 × 0.20 × 0.30	0.20 × 0.25 × 0.45	0.50 × 0.35 × 0.25	0.15 × 0.20 × 0.45	0.15 × 0.25 × 0.50	0.60 × 0.40 × 0.40
cryst syst	orthorhombic	orthorhombic	monoclinic	triclinic	monoclinic	monoclinic
space group	<i>Pbca</i> (no.61)	<i>Pbca</i> (no.61)	<i>P2₁/c</i> (no.14)	<i>P1</i> (no.2)	<i>P2₁</i> (no.4)	<i>P2₁/c</i> (no.14)
<i>a</i> , Å	18.2743(9)	18.167(1)	12.0991(3)	11.7461(9)	11.1570(4)	20.2123(5)
<i>b</i> , Å	26.993(1)	26.5525(4)	16.3568(3)	13.433(2)	21.4652(14)	18.8132(4)
<i>c</i> , Å	27.782(2)	27.6449(2)	18.2721(5)	15.608(2)	19.3730(3)	21.0448(4)
α, deg	90	90	90	70.409(5)	90	90
β, deg	90	90	103.283(2)	87.346(3)	104.9780(3)	113.675(2)
γ, deg	90	90	90	65.5352(13)	90	90
<i>V</i> , Å ³	13704(1)	13335.2(6)	3519.4(1)	2099.5(4)	4482.0(3)	7329.0(3)
<i>Z</i>	8	8	2	1	4	8
ρ _{calcd} , g cm ⁻³	1.274	1.481	1.462	1.299	1.218	1.419
<i>F</i> (000)	5472.00	5984.00	1576.00	862.00	1740.00	3176.00
μ(Mo, Kα), cm ⁻¹	20.31	32.97	25.00	16.10	15.11	27.91
total no. of reflns	114 732	122 553	30 341	20 180	42 041	62 012
no. of unique reflns	23 388	17 131	7754	10 065	11 099	16 219
<i>R</i> _{int}	0.078	0.048	0.035	0.045	0.070	0.039
reflns with <i>I</i> ≥ 3σ(<i>I</i>)	6235	8414	6375	5868	13 899	11 481
no. of variables	613	613	352	459	864	703
<i>R</i> (<i>F</i> , <i>I</i> ≥ 3σ(<i>I</i>))	0.060	0.080	0.023	0.086	0.114	0.033
<i>R</i> _w (<i>F</i> , <i>I</i> ≥ 3σ(<i>I</i>))	0.056	0.081	0.030	0.079	0.146	0.047
<i>R</i> (<i>F</i> ² , all data)	0.106	0.139	0.043	0.046	0.062	0.063
<i>R</i> _w (<i>F</i> ² , all data)	0.125	0.180	0.066	0.036	0.073	0.104
gof	1.91	2.68	1.26	1.72	1.33	1.37
max Δ/σ (final cycle)	0.002	0.005	0.01	0.06	0.04	0.06
residual density, e Å ⁻³	-1.14 to +2.57	-5.25 to +11.18 (near Lu)	-1.19 to +1.62	-1.27 to +1.06	-2.53 to +4.93	-1.51 to +4.37

colored complexes of yttrium(III) [P₂N₂] (P₂N₂ = PhP(CH₂-SiMe₂NSiMe₂CH₂)₂PPh) upon reaction with aryllithium reagents.²⁰ We have traced the origin of the color to the formation of biphenyldiide derivatives via an intriguing carbon-carbon bond coupling reaction that does not require any change of formal oxidation state nor involve any migratory insertion chemistry. In this paper we detail our studies to understand these reactions, in particular, to probe the effect of changing the metal from yttrium(III) to other members of group 3 and to the lanthanides. What becomes apparent is that the formation of carbon-carbon bonds via this process is very dependent on the size of the metal ion.

Results and Discussion

Synthesis and Structure of {[P₂N₂]M}₂(μ-Cl)₂ 1a-e. The starting materials for all of the chemistry described for these group 3 and lanthanide complexes are the chloride-bridged dimers {[P₂N₂]M}₂(μ-Cl)₂ (M = Y, Sm, Ho, Yb, Lu) **1a-e**, which can be synthesized in high to quantitative yields by the reaction of *syn*-Li₂-(dioxane)[P₂N₂] with MCl₃(THF)₃ in toluene at 85 °C. They are isolated as colorless or pale-colored solids. For **1a** and **1e**, crystals suitable for X-ray diffraction were grown; the molecular structure of **1a** is shown in Figure 1; crystal data are given in Table 1 and selected bond lengths and angles for **1a** and **1e** in Tables 2 and 3, respectively. The complexes are isostructural and contain two structurally different metal centers joined with bridging chloride ligands; M1 resides in a distorted trigonal prismatic environment, while the geometry of M2 is distorted octahedral. In contrast to the solid-state structures, the diamagnetic species **1a** and **1e** show solution NMR spectra that indicate both ends of the molecule are equivalent; thus the previously observed¹⁵

Table 2. Selected Bond Lengths (Å) and Angles (deg) in {[P₂N₂]Y}₂(μ-Cl)₂, **1a**

Y(1)-N(1)	2.270(3)	Y(1)-N(2)	2.283(3)
Y(1)-P(1)	2.827(1)	Y(1)-P(2)	2.844(1)
Y(2)-N(3)	2.255(3)	Y(2)-N(4)	2.274(3)
Y(2)-P(3)	2.895(1)	Y(2)-P(4)	2.904(1)
Y(1)-Cl(1)	2.697(1)	Y(1)-Cl(2)	2.707(1)
Y(2)-Cl(1)	2.708(1)	Y(2)-Cl(2)	2.730(1)
Cl(1)-Y(1)-Cl(2)	77.05(3)	Cl(1)-Y(1)-P(1)	96.67(4)
Cl(1)-Y(1)-P(2)	98.35(4)	Cl(1)-Y(1)-N(1)	91.90(9)
Cl(1)-Y(1)-N(2)	169.36(9)	Cl(2)-Y(1)-P(1)	92.59(4)
Cl(2)-Y(1)-P(2)	103.00(4)	Cl(2)-Y(1)-N(1)	92.59(4)
Cl(2)-Y(1)-N(2)	92.31(9)	N(1)-Y(1)-N(2)	98.7(1)
P(1)-Y(1)-P(2)	160.38(4)		
Cl(1)-Y(2)-Cl(2)	76.47(3)	Cl(1)-Y(2)-P(3)	86.14(4)
Cl(1)-Y(2)-P(4)	130.45(4)	Cl(1)-Y(2)-N(3)	98.07(9)
Cl(1)-Y(2)-N(4)	143.43(9)	Cl(2)-Y(2)-P(3)	129.37(4)
Cl(2)-Y(2)-P(4)	86.76(4)	Cl(2)-Y(2)-N(3)	147.38(9)
Cl(2)-Y(2)-N(4)	95.83(9)	N(3)-Y(2)-N(4)	106.1(1)
P(3)-Y(2)-P(4)	136.69(4)		

flexibility of the [P₂N₂] ligand framework allows approximately C_{2v} symmetry in solution. In particular, two silylmethyl environments are observed in the ¹H NMR spectrum, and in the ³¹P{¹H} NMR spectrum, a single phosphorus environment is observed: for **1a** a doublet at -33.8 ppm (*J*_{YP} = 84.0 Hz) and for **1e** a singlet at -26.0 ppm. The Sm, Ho, and Yb derivatives (**1b-d**) are paramagnetic species as anticipated; only broadened, contact-shifted resonances are observed in the ¹H NMR spectrum, which could not be interpreted due to overlapping and missing resonances.

Aryl Coupling Reactions at Yttrium. The impetus for this project arose out of the observation of deep blue solutions that resulted when the colorless yttrium(III) alkyl complex [P₂N₂]Y(CH₂SiMe₃), **2a**, was dissolved in aromatic solvents such as benzene. Once the biphenyldiide complex {[P₂N₂]Y}₂{μ-η⁶:η⁶-(C₆H₅)₂}, **3a**, was structurally characterized,²⁰ we recognized that a more direct route to these complexes was via the reaction of PhLi

(20) Fryzuk, M. D.; Love, J. B.; Rettig, S. J. *J. Am. Chem. Soc.* **1997**, *119*, 9071.

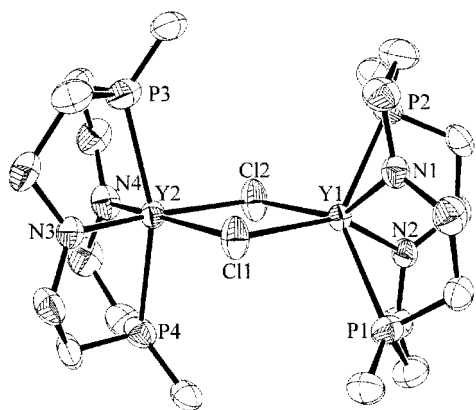
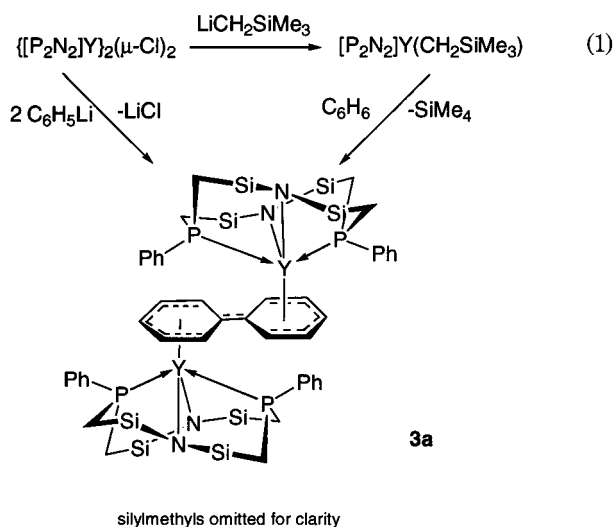


Figure 1. ORTEP representation of the solid state molecular structure of $\{[P_2N_2]Y\}_2(\mu\text{-Cl})_2$, **1a**.

Table 3. Selected Bond Lengths (Å) and Angles (deg) in $\{[P_2N_2]Lu\}_2(\mu\text{-Cl})_2$, **1e**

Lu(1)–N(1)	2.231(7)	Lu(1)–N(2)	2.200(8)
Lu(1)–P(1)	2.785(2)	Lu(1)–P(2)	2.795(2)
Lu(2)–N(3)	2.229(7)	Lu(2)–N(4)	2.270(7)
Lu(2)–P(3)	2.855(2)	Lu(2)–P(4)	2.847(2)
Lu(1)–Cl(1)	2.654(2)	Lu(1)–Cl(2)	2.665(2)
Lu(2)–Cl(1)	2.671(2)	Lu(2)–Cl(2)	2.692(2)
Cl(1)–Lu(1)–Cl(2)	77.27(7)	Cl(1)–Lu(1)–P(1)	95.20(8)
Cl(1)–Lu(1)–P(2)	98.83(8)	Cl(1)–Lu(1)–N(1)	168.2(2)
Cl(1)–Lu(1)–N(2)	91.7(2)	Cl(2)–Lu(1)–P(1)	93.86(8)
Cl(2)–Lu(1)–P(2)	100.27(8)	Cl(2)–Lu(1)–N(1)	90.9(2)
Cl(2)–Lu(1)–N(2)	168.6(2)	N(1)–Lu(1)–N(2)	100.1(3)
P(1)–Lu(1)–P(2)	161.94(9)		
Cl(1)–Lu(2)–Cl(2)	76.52(7)	Cl(1)–Lu(2)–P(3)	128.27(8)
Cl(1)–Lu(2)–P(4)	86.26(7)	Cl(1)–Lu(2)–N(3)	96.3(2)
Cl(1)–Lu(2)–N(4)	144.8(2)	Cl(2)–Lu(2)–P(3)	87.17(7)
Cl(2)–Lu(2)–P(4)	127.35(8)	Cl(2)–Lu(2)–N(3)	148.6(2)
Cl(2)–Lu(2)–N(4)	95.2(2)	N(3)–Lu(2)–N(4)	106.8(3)
P(3)–Lu(2)–P(4)	138.55(7)		

with the chloride-bridged dimer **1a**. Reaction of 2.2 equiv of aryllithium with **1a** in toluene at -78°C , followed by additional stirring at room temperature, affords blue solutions of the coupled diaryl complex (eq 1) in modest yields.



The reaction of *m*-tolyllithium with **1a** also produced a dark blue complex, $\{[P_2N_2]Y\}_2\{\mu\text{-}\eta^6\text{-}\eta^6\text{-}(\text{C}_6\text{H}_4\text{-}m\text{-Me})_2\}$,²⁰ which although not structurally characterized, was shown to be a π -biphenyl-bridged dimer by analogy

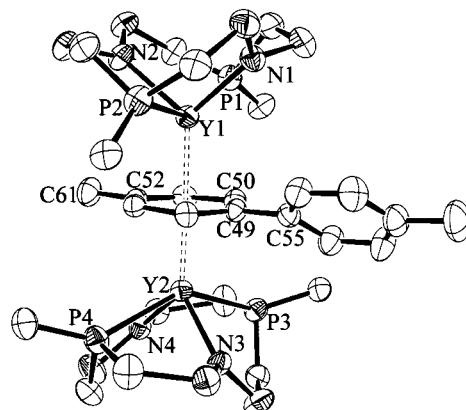


Figure 2. ORTEP representation of the solid state molecular structure of $\{[P_2N_2]Y\}_2\{\mu\text{-}\eta^6\text{:}\eta^6\text{-C}_6\text{H}_4\text{-}p\text{-Me}\}(\text{C}_6\text{H}_4\text{-}p\text{-Me})$, **4** (from ref 20).

to **3a** using NMR spectroscopic data. The reaction of **1a** with *p*-tolyllithium gave a brown product whose structure showed the $[P_2N_2]Y$ fragments bound to the same ring (on opposite faces) with the remaining ring uncoordinated and retaining its aromaticity, Figure 2.²⁰

Interestingly, the solution ^1H NMR data for **4** are inconsistent with this solid state structure, as resonances for only one type of coordinated *p*-tolyl group are observed at room temperature; therefore, the $[P_2N_2]Y$ fragments must be migrating across the π -surface of the bi-*p*-tolyl diide moiety on the NMR time scale. In support of this proposal, at -95°C broad resonances for an uncoordinated arene are observed between 6 and 7 ppm, in addition to high-field-shifted resonances for the sandwiched *p*-tolyl moiety; this suggests that the solid state structure represents a low-temperature limiting structure for this process. This type of dynamic behavior probably occurs to some extent in all $[P_2N_2]Y$ biaryldiide complexes, even **3a**; however, we were unable to reach a low-temperature limiting structure with **3a** or any other of these coupled diaryl products.

The above reactions of simple aryllithium reagents (i.e., phenyllithium, *m*-tolyllithium, and *p*-tolyllithium) **1a** show how small changes can affect the structure of the coupled diaryl products.²⁰ In an effort to examine this further, other *p*-substituted-aryllithium reagents were allowed to react with **1a**; *p*-*tert*-butylphenyllithium, *p*-chlorophenyllithium, *p*-methoxyphenyllithium, and *p*-trifluoromethylphenyllithium did not result in the formation of any coupled diaryl derivatives. Analysis of the crude products showed that mixtures of products were formed that defied characterization; in addition, no deep colors were observed indicative of coupled diaryls. However, one substituted aryllithium reagent was eventually found to undergo this process. The reaction of biphenyllithium (*p*-Ph- $\text{C}_6\text{H}_4\text{Li}$) with **1a** generated dark blue crystals of the bisbiphenyl-coupled product **5**. X-ray structure analysis of **5** was undertaken and it showed a bisbiphenyl moiety sandwiched by two $[P_2N_2]Y$ units that are η^6 -coordinated to the two middle rings. The solid state molecular structure of $\{[P_2N_2]Y\}_2\{\mu\text{-}\eta^6\text{:}\eta^6\text{-}(\text{C}_6\text{H}_4\text{-}p\text{-Ph})_2\}$ (**5**) is shown in Figure 3, and selected bond lengths and bond angles are shown in Table 4. The C–C bond distance between the two coordinated rings is 1.396(6) Å, which indicates a double bond. The C–C bond distances between the coordinated and the non-

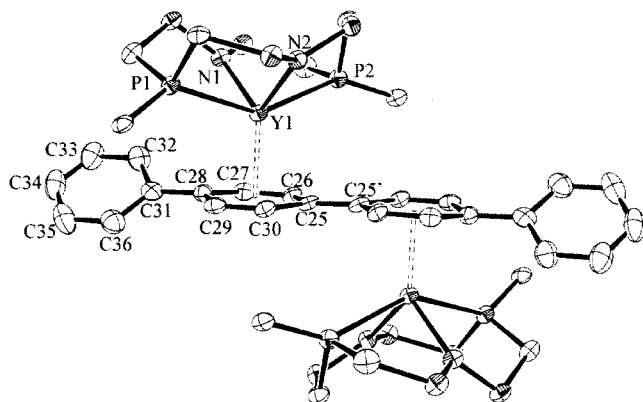


Figure 3. ORTEP representation of the solid state molecular structure of $\{[P_2N_2]Y\}_2\{\mu\text{-}\eta^6\text{:}\eta^6\text{-}(C_6H_4\text{-}p\text{-}Ph)_2\}$, **5**.

Table 4. Selected Bond Lengths (Å) and Angles (deg) in $\{[P_2N_2]Y\}_2\{\mu\text{-}\eta^6\text{:}\eta^6\text{-}(C_6H_4\text{-}p\text{-}Ph)_2\}$, **5**

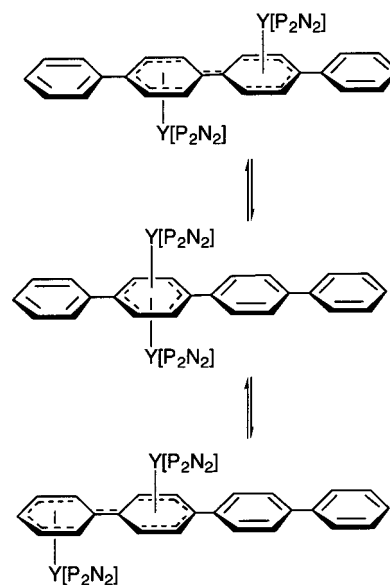
Y(1)–N(1)	2.304(2)	Y(1)–N(2)	2.299(2)
Y(1)–P(1)	2.9267(10)	Y(1)–P(2)	2.9075(10)
Y(1)–C(25)	2.737(3)	Y(1)–C(26)	2.726(3)
Y(1)–C(27)	2.716(3)	Y(1)–C(28)	2.705(3)
Y(1)–C(29)	2.765(3)	Y(1)–C(30)	2.730(3)
C(25)–C(25)	1.396(6)	C(25)–C(26)	1.474(4)
C(26)–C(27)	1.374(4)	C(27)–C(28)	1.407(5)
C(28)–C(29)	1.444(4)	C(29)–C(30)	1.370(4)
C(25)–C(30)	1.458(5)	C(28)–C(31)	1.464(5)
C(31)–C(32)	1.420(5)	C(32)–C(33)	1.379(5)
C(33)–C(34)	1.368(6)	C(34)–C(35)	1.394(6)
C(35)–C(36)	1.382(5)	C(31)–C(36)	1.400(5)
N(1)–Y(1)–N(2)	101.97(9)	P(1)–Y(1)–P(2)	146.81(3)

coordinated rings are in the range of a single bond at 1.464(5) Å. The C–C bond distances in the coordinated rings are inequivalent, but are similar to those shown in the biphenyl analogue, **3a**.²⁰ The aromaticity is preserved in the outer noncoordinated rings, as is evident by the equivalent C–C bond lengths. The two coordinated rings are coplanar, but each is twisted by 32.5° from its neighboring noncoordinated ring. Therefore, the two inner rings can be considered as a biphenyl dianion with each ring substituted by a phenyl ring at the *para*-position. The average Y–C(ring) bond distance is 2.730(3) Å, identical to that in **3a**.

X-ray analysis clearly shows the presence of two types of rings, one coordinated to the metal center and no longer aromatic, and the other noncoordinated and aromatic. Five upfield-shifted resonances in the ¹H NMR spectrum were attributed to the π -bonded bisphenyl protons at 6.50, 6.40, 6.20, 5.80, and 5.50 ppm, and no resonances that correspond to uncoordinated phenyl groups were observed. The room-temperature ³¹P{¹H} NMR spectrum exhibits a doublet at –26.87 ppm ($J_{YP} = 84.1$ Hz) that is consistent with equivalent phosphorus environments. The implication is that, in solution, there is a fluxional process in which the two $[P_2N_2]Y$ units traverse the π -surfaces of all four of the rings, as illustrated in Scheme 1. If such a process occurs rapidly on the NMR time scale, one can anticipate that all four rings will experience some upfield shielding due to the presence of the coordinated yttrium center.

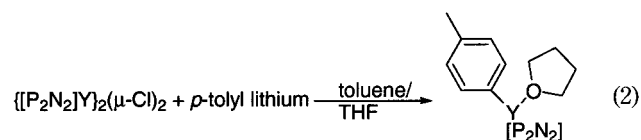
This type of rapid fluxional process was also observed for $[P_2N_2]Ln$ cations coordinated to polyaromatic ligands.²¹ As with those examples, attempts to freeze out this process were unsuccessful. As the tempera-

Scheme 1. Fluxional Behavior of **5**



ture of a C₇D₈ solution of **5** was lowered, the signals due to the bisphenyl moiety started to broaden and gave rise to three resonances at 6.71, 5.90, and 5.47 ppm. At –15 °C a single broad resonance was observed between 6.50 and 5.00 ppm, but there was no evidence for less symmetric products despite cooling to –60 °C. The ³¹P{¹H} NMR spectra in the same temperature range exhibited single broad resonances: –27.8 ppm ($\nu_{1/2} = 180$ Hz, –15 °C) and –28.5 ppm ($\nu_{1/2} = 400$ Hz, –30 °C).

In all of the reactions of **1a** with aryllithiums that have been discussed above, the solvent system of choice was toluene, sometimes in the presence of diethyl ether. To examine the effect of using a highly coordinating solvent upon the course of reaction, **1a** was allowed to react with *p*-tolyl lithium in a solvent mixture of toluene and THF (eq 2). Evaporating the solvents caused no color change, and a white microcrystalline solid, **6**, was isolated after workup. The ¹H NMR spectrum of this compound did not show any signals due to a π -coordinated *p*-tolyl ring. Instead, a singlet due to the methyl group of the *p*-tolyl moiety occurs at 2.40 ppm, and the protons of the *p*-tolyl ring appear as a multiplet at 7.23 ppm. Two broad resonances due to the coordinated THF are observed at 3.80 and 1.29 ppm. The ³¹P{¹H} NMR spectrum shows a doublet at –33.9 ppm ($J_{YP} = 56$ Hz).



The X-ray crystal structure of **6** shows that the complex is mononuclear with yttrium coordinated to a $[P_2N_2]$ moiety and a THF molecule and also σ -coordinated to a *p*-tolyl group. The coordination geometry around the yttrium center is distorted trigonal prismatic. The Y–C bond distance, 2.472(6) Å, is longer

(21) Fryzuk, M. D.; Jafarpour, L.; Kerton, F. M.; Love, J. B.; Rettig, S. J. *Angew. Chem., Int. Ed.* **2000**, *39*, 767.

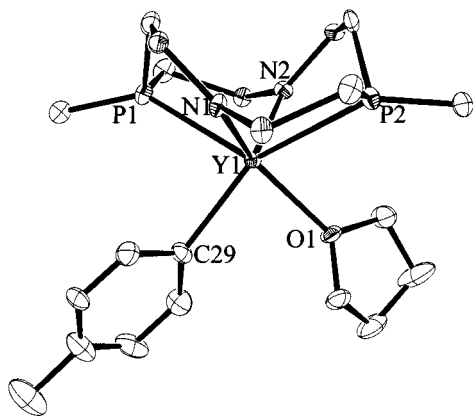


Figure 4. ORTEP representation of the solid state molecular structure of $[\text{P}_2\text{N}_2]\text{Y}(\text{C}_6\text{H}_4\text{-}p\text{-Me})(\text{THF})$, **6**.

Table 5. Selected Bond Lengths (Å) and Angles (deg) in $[\text{P}_2\text{N}_2]\text{Y}(\text{C}_6\text{H}_4\text{-}p\text{-Me})(\text{THF})$, **6**

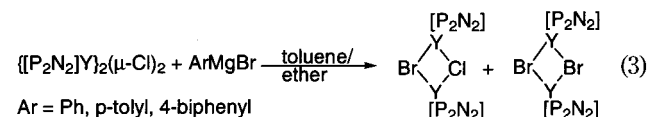
Y(1)–N(1)	2.283(4)	Y(1)–N(2)	2.321(5)
Y(1)–P(1)	2.9396(15)	Y(1)–P(2)	3.0391(15)
Y(1)–O(1)	2.401(4)	Y(1)–C(29)	2.472(6)
N(1)–Y(1)–N(2)	109.8(2)	P(1)–Y(1)–P(2)	126.05(5)

than that of 2.394(6) Å found for the σ -bonded complex, $[\text{P}_2\text{N}_2]\text{Y}\{\text{CH}(\text{SiMe}_3)_2\}$,²⁰ and shorter than the yttrium to arene carbon bonds in **2a** that range from 2.629(4) to 2.699(4) Å. Therefore, the presence of a strongly coordinating molecule such as THF blocks the C–C bond coupling reaction. The solid state molecular structure of **6** is shown in Figure 4, and selected bond lengths and angles are shown in Table 5.

If the coordinated THF molecule could be removed from the coordination sphere of the Y center, it would open up a coordination site that might facilitate the formation of **3a** via coupling. Cyclic ethers undergo electrophilic attack with ring opening when treated with trimethylsilyliodide.²² This property of Me_3SiI was used to remove the THF ligand from $\text{Cp}^*\text{La}\{\text{CH}(\text{SiMe}_3)_2\}_2(\text{THF})$.²³ Reacting **6** with excess Me_3SiI results in ring opening of the coordinated THF, as seen in the ^1H NMR spectrum along with formation of $\{[\text{P}_2\text{N}_2]\text{Y}\}_2(\mu\text{-I})_2$ and some intractable materials. Treating **6** with only 1 equiv of Me_3SiI did not result in THF ring opening. Attempts to use Lewis acids such as AlPh_3 and $\text{B}(\text{C}_6\text{F}_5)_3$ to remove the THF were unsuccessful; in these latter reactions, no reaction occurred and the starting materials were recovered.

When **1a** was allowed to react with Grignard reagents such as PhMgBr , $p\text{-tolylMgBr}$, and $p\text{-biphenylMgBr}$, the formation of white precipitates was not observed, and the colorless reaction mixture did not change color when the diethyl ether solvent was evaporated; workup of these reactions produced white solids. The $^{31}\text{P}\{^1\text{H}\}$ NMR spectra of these products were identical for all three cases with three doublets at -33.3 ($J_{\text{YP}} = 83.3$ Hz), -33.45 ($J_{\text{YP}} = 82.7$), and -33.55 ppm ($J_{\text{YP}} = 83$ Hz). The first doublet is the starting chloride **1a**, and the other two are the products of halide exchange, namely, $\{[\text{P}_2\text{N}_2]\text{Y}\}_2(\mu\text{-Cl})(\mu\text{-Br})$ and $\{[\text{P}_2\text{N}_2]\text{Y}\}_2(\mu\text{-Br})_2$, as shown in eq 3. Increasing the temperature

and the reaction time did not change the outcome of these reactions.



Aryl Coupling Reactions of the Lanthanides.

Having successfully obtained the $[\text{P}_2\text{N}_2]\text{Y}$ -coupled diaryl complexes by reacting **1a** with phenyl, *m*-tolyl, *p*-tolyl, and biphenyllithium reagents, we set out to prepare the lutetium analogues by reaction with $\{[\text{P}_2\text{N}_2]\text{Lu}\}_2(\mu\text{-Cl})_2$, **1e**. However, the formation of highly colored solutions was not observed in any experiment, and only white solids were isolated. These were only sparingly soluble in hydrocarbon and aromatic solvents. Therefore attempts to obtain NMR spectra in C_6D_6 or C_7D_8 were futile. The noncoordinating polar solvent CD_2Cl_2 reacted with the complex to afford the free ligand $[\text{P}_2\text{N}_2\text{D}_2]$ and an insoluble white powder, presumably YCl_3 . Interpretable NMR spectra could be obtained from $\text{C}_4\text{D}_8\text{O}$ solutions. It is assumed that *ate* complexes are present, as a single resonance at -0.7 ppm ($\nu_{1/2} = 15$ Hz, 27°C) is observed in the ^7Li NMR spectrum of all samples in saturated $\text{C}_4\text{D}_8\text{O}$ solutions. The frequency compares well with that reported for $\text{La}(\text{CH}\{\text{SiMe}_3\}_2)_3(\mu\text{-Cl})\text{Li}(\text{pm-deta})$, -0.2 ppm.²⁴ Two anions are presumably present, possibly $\{[\text{P}_2\text{N}_2]\text{LuPh}_2\}^-$ and $\{[\text{P}_2\text{N}_2]\text{LuCl}_2\}^-$, as two different ^{31}P environments are observed at -18.7 and -20.3 ppm in a ratio of 1:1 and for the *p*-tolyl derivative -19.3 and -20.9 ppm. The presence of two anions is also evident in the ^1H NMR spectrum, where eight SiMe_2 environments are observed, along with many overlapping multiplets in the aromatic region. No change in appearance of the NMR spectra was observed over a temperature range of -70 to 80°C . Elemental analysis of the white powder showed a lower level of C and a higher level of N than expected; this is probably due to incomplete combustion of the sample and is not uncommon in organometallic lanthanide complexes.^{25,26} Attempts to isolate the Lu analogue of the THF adduct **6** upon performing the reaction in THF were unsuccessful; removal of the solvent in vacuo afforded the hydrocarbon-insoluble white powder identical to that described above. Attempts to obtain crystals of these Lu complexes have been frustrated by their low solubility. However, their coloration when compared with **3a–c** and **5** and the lack of high-field-shifted arene protons in the ^1H NMR spectra indicate the formation of σ -bonded complexes, and no evidence for C–C bond formation is apparent. No reaction occurred when PhMgBr was allowed to react with the lutetium chloro-bridged dimer **1e** even after 1 week.

It had previously been shown by our group that dinuclear $[\text{P}_2\text{N}_2]\text{Lu}$ polycyclic aromatic π -complexes could be prepared via a reductive route.²¹ This route is successful for the preparation of $\{[\text{P}_2\text{N}_2]\text{Lu}\}_2\{\mu\text{-}\eta^6\text{:}\eta^6\text{-}(\text{C}_6\text{H}_5)_2\}$, **3e**, which can be isolated as a crystalline blue

(24) Atwood, J. L.; Lappert, M. F.; Smith, R. G.; Zhang, H. *Chem. Commun.* **1988**, 1308.

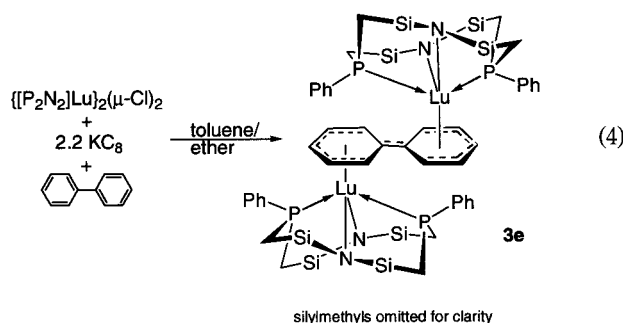
(25) Qian, C. T.; Nie, W. L.; Sun, J. *J. Chem. Soc., Dalton Trans.* **1999**, 3283.

(26) Eppinger, J.; Spiegler, M.; Hieringer, W.; Herrmann, W. A.; Anwander, R. *J. Am. Chem. Soc.* **2000**, *122*, 3080.

(22) Olah, G. A.; Narang, S. C. *Tetrahedron* **1982**, *38*, 2225.

(23) van der Heijden, H.; Schaverien, C. J. *Organometallics* **1989**, *8*, 255.

solid in moderate yields via the reaction of **1e** with biphenyl in the presence of KC_8 (eq 4).



The ^1H NMR spectrum of **3e** contains three upfield-shifted resonances, which are attributed to the π -bonded biphenyl protons at 5.04, 4.41, and 4.03 ppm. The $^{31}\text{P}\{-^1\text{H}\}$ NMR spectrum exhibits equivalent phosphorus environments, with a singlet at -15.4 ppm. The solution NMR data and the distinctive blue color of the material are consistent with a structure that is identical to the yttrium and holmium biphenyldiide complexes **3a** and **3c**. This reductive route could also be used to prepare the yttrium analogue **3a**, albeit in lower yields than those obtained via the PhLi route.

The isolation of $\{[\text{P}_2\text{N}_2]\text{Lu}\}_2\{\mu\text{-}\eta^6\text{-}\eta^6\text{-(C}_6\text{H}_5)_2\}$ via the reaction of biphenyl under reducing conditions suggests that the inability of the lutetium complex to undergo the coupling reaction is a kinetic effect and not because of any thermodynamic instability of the ultimate product. The smaller size of lutetium(III) compared to yttrium(III) may prevent the putative, but crucial phenyl-bridged dimer formation that is suggested to be necessary for aryl coupling (vide infra).

Reaction of PhLi with $\{[\text{P}_2\text{N}_2]\text{Yb}\}_2(\mu\text{-Cl})_2$ (**1d**) in toluene proceeded with a color change from yellow to dark green. Extraction of the crude green product with hexanes and cooling to -30 °C resulted in the isolation of the mononuclear σ -phenyl complex $[\text{P}_2\text{N}_2]\text{Yb}(\text{C}_6\text{H}_5)$ (**8**) as orange crystals in modest yield. The green byproduct could be the bridged biphenyl dimer, although we were unable to confirm this experimentally. Heating the mononuclear phenyl derivative **8** to 110 °C in toluene for 48 h resulted in no color change and therefore no coupling. The isolation of this mononuclear σ -phenyl complex, which is unobtainable for the Y series, indicates an increased stability for this species possibly due to the smaller size of the metal.

The solid state molecular structure of **8** is shown in Figure 5, and selected bond lengths and bond angles are shown in Table 6.

Two molecules are present in the asymmetric unit cell; in both there is significant thermal motion associated with the Yb-bound phenyl ring. However, this motion could not be well refined as simple static disorder, and as such, the positions of the hydrogen atoms could not be refined. In both molecules the Yb is in a distorted square-pyramidal environment with the four N and P atoms in the basal plane and C25 in the apical position. The Yb–C bond distances are 2.336(5) and 2.351(5) Å; only a limited number of Yb complexes, or indeed crystallographically characterized Ln complexes, with σ -bonded aryl ligands have been synthesized to date.²⁷ Homoleptic complexes such as Ph_2Yb

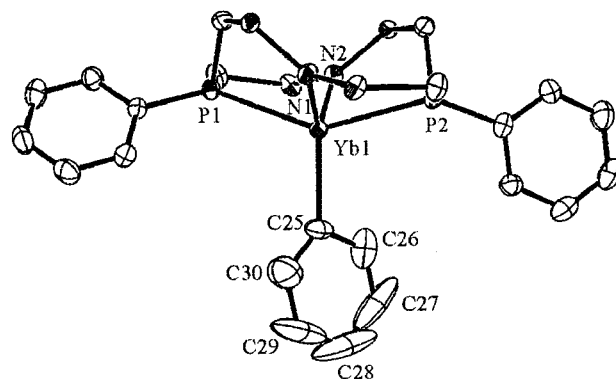


Figure 5. ORTEP representation of the solid state molecular structure of $[\text{P}_2\text{N}_2]\text{YbPh}$, **8**.

Table 6. Selected Bond Lengths (Å) and Angles (deg) in $[\text{P}_2\text{N}_2]\text{Yb}(\text{C}_6\text{H}_5)$, **8**

Yb(1)–N(1)	2.220(4)	Yb(1)–N(2)	2.230(3)
Yb(2)–N(3)	2.234(4)	Yb(2)–N(4)	2.240(4)
Yb(1)–P(1)	2.810(1)	Yb(1)–P(2)	2.809(1)
Yb(2)–P(3)	2.825(1)	Yb(2)–P(4)	2.804(1)
Yb(1)–C(25)	2.336(5)	Yb(2)–C(55)	2.351(5)
N(1)–Yb(1)–N(2)	110.0(1)	P(1)–Yb(1)–P(2)	145.65(3)
N(3)–Yb(2)–N(4)	111.5(1)	P(3)–Yb(2)–P(4)	143.11(4)
N(1)–Yb(1)–C(25)	124.4(2)	N(2)–Yb(1)–C(25)	125.5(2)
N(3)–Yb(2)–C(55)	122.9(2)	N(4)–Yb(2)–C(55)	125.6(2)
P(1)–Yb(1)–C(25)	109.9(1)	P(2)–Yb(1)–C(25)	104.4(1)
P(3)–Yb(2)–C(55)	108.5(1)	P(4)–Yb(2)–C(55)	108.4(1)
Yb(1)–C(25)–C(26)	111.6(4)	Yb(1)–C(25)–C(30)	134.3(5)
Yb(2)–C(55)–C(56)	118.9(4)	Yb(2)–C(55)–C(60)	127.3(4)

(THF)₃ and $\text{Ph}_2(\text{THF})\text{Yb}(\mu\text{-Ph})_3\text{Yb}(\text{THF})_3$ have comparable bond distances for their terminal phenyl groups, 2.39–(1)–2.463(32) Å.^{28,29} Recently, the 2,6-dimesitylphenyl ligand has been used successfully in the presence of other ligands, but due to the steric demand of this ligand, the Yb–C bond distances are significantly longer, 2.403(4)–2.447(9) Å, than in our example.^{30,31} The intramolecular Yb–H bond distances for the *ortho* protons of the phenyl groups are Yb(1)–H(43) 2.987 Å, Yb(1)–H(47) 3.587 Å, Yb(2)–H(90) 3.202 Å, and Yb(2)–H(96) 3.466 Å. Although not refined, there is clearly some evidence of an agostic interaction in molecule 1, namely, the C(26)–H(43) bond and Yb(1). This is also evident when comparing bond angles around the Yb bound C atoms: Yb(1)–C(25)–C(26) 111.6(4)° and Yb(1)–C(25)–C(30) 134.3(5)°, Yb(2)–C(55)–C(56) 118.9(4)°, and Yb(2)–C(55)–C(60) 127.3(4)°; there is clearly a tilt of the Ph ring toward one side of the molecule away from the planes containing either the N atoms and Yb or the P atoms and Yb.

The reaction of **1e**, $\{[\text{P}_2\text{N}_2]\text{Sm}\}_2(\mu\text{-Cl})_2$, and also $\{[\text{P}_2\text{N}_2]\text{Ln}\}_2(\mu\text{-I})_2$, Ln = Sm, La, with PhLi in toluene proceeded with a darkening of color to afford dark purple/brown solutions. However, the hexanes extract from these reactions afforded upon cooling colorless crystals of $\text{Li}_2[\text{P}_2\text{N}_2]$. The identity of the dark-colored complexes are yet to be confirmed; however, one pos-

(27) Cotton, S. A. *Coord. Chem. Rev.* **1997**, *160*, 93.

(28) Bochkarev, M. N.; Khramenkov, V. V.; Rad'kov, Y. F.; Zakharov, L. N.; Struchkov, Y. T. *J. Organomet. Chem.* **1992**, *429*, 27.

(29) Zakharov, L. N.; Struchkov, Y. T. *J. Organomet. Chem.* **1997**, *536*, 65.

(30) Rabe, G. W.; Strissel, C. S.; Liable-Sands, L. M.; Concolino, T. E.; Rheingold, A. L. *Inorg. Chem.* **1999**, *38*, 3446.

(31) Niemeyer, M.; Hauber, S.-O. *Z. Anorg. Allg. Chem.* **1999**, *625*, 137.

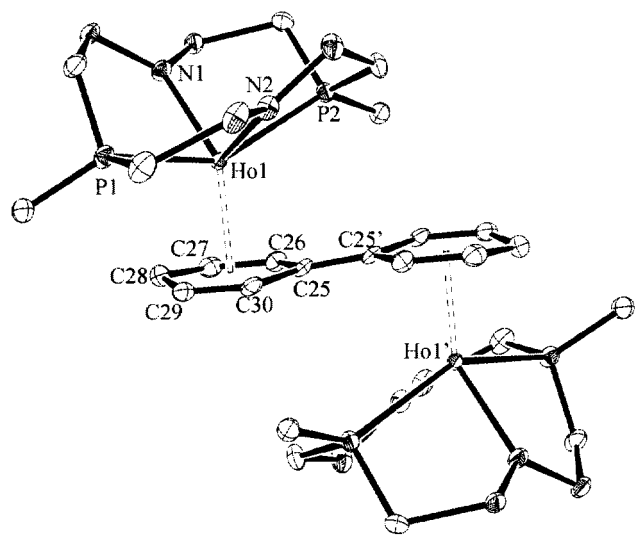


Figure 6. ORTEP representation of the solid state molecular structure of $\{[P_2N_2]Ho\}_2\{\mu\text{-}\eta^6\text{:}\eta^6\text{-}(C_6H_5)_2\}$, **3c**.

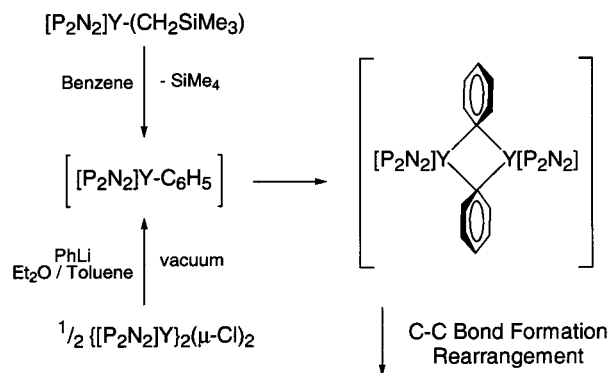
Table 7. Selected Bond Lengths (Å) and Angles (deg) in $\{[P_2N_2]Ho\}_2\{\mu\text{-}\eta^6\text{:}\eta^6\text{-}(C_6H_5)_2\}$, **3c**

Ho(1)–N(1)	2.313(2)	Ho(1)–N(2)	2.322(2)
Ho(1)–P(1)	2.9229(6)	Ho(1)–P(2)	2.8000(6)
Ho(1)–C(25)	2.688(2)	Ho(1)–C(26)	2.708(2)
Ho(1)–C(27)	2.731(2)	Ho(1)–C(28)	2.666(2)
Ho(1)–C(29)	2.737(2)	Ho(1)–C(30)	2.718(2)
C(25)–C(25)	1.403(5)	C(25)–C(26)	1.460(4)
C(26)–C(27)	1.363(4)	C(27)–C(28)	1.425(4)
C(28)–C(29)	1.418(4)	C(29)–C(30)	1.375(4)
C(25)–C(30)	1.464(3)		
N(1)–Ho(1)–N(2)	99.42(8)	P(1)–Ho(1)–P(2)	149.19(2)

sibility is the formation of $\{Ml_2(THF)_n\}_2\{\mu\text{-}\eta^6\text{:}\eta^6\text{-}(C_6H_5)_2\}$ or similar species. Several complexes of this type have been previously reported:^{32,33} $\{LaI_2(THF)_3\}_2\{\mu\text{-}\eta^4\text{:}\eta^4\text{-}C_{10}H_8\}$ and $\{LaI_2(THF)_3\}_2\{\mu\text{-}\eta^4\text{:}\eta^4\text{-}s\text{-}cis\text{-}PhCH\text{-}CHCH\text{-}CPh\}$.

The reaction of the holmium chloro-bridged dimer **1c** with PhLi in toluene proceeded with a color change from colorless to blue, and from this reaction a mixture of blue crystals of **3c** could be isolated. **3c** can also be synthesized via a σ -bond metathesis reaction of benzene and the trimethylsilylmethyl derivative $[P_2N_2]Ho\text{-}(CH_2SiMe_3)$, **2c**, in the same way as that observed for the Y analogue.²⁰ The solid state molecular structure of **3c** is shown in Figure 6, and selected bond lengths and bond angles are shown in Table 7; it is isostructural with **3a**.²⁰ The structure of **3c** shows a bridging biphenyl moiety sandwiched by two $[P_2N_2]Ho$ units that are η^6 -coordinated to each ring. The C–C bond distance between the two coordinated rings is 1.403(5) Å, which is shorter than a single bond and comparable with that previously observed in **3a** (1.393(8) Å).²⁰ The C–C bond distances in the coordinated rings are inequivalent [1.363(4)–1.456(5) Å], but are similar to those shown in the yttrium analogue, **3a**.²⁰ Therefore, the two planar rings can be considered as a biphenyl dianion. The planarity of the rings is worthy of note, as other polyaromatics, such as naphthalene, have been found to undergo puckering distortions upon coordination to

Scheme 2. Proposed Mechanism for C–C Bond Formation by $[P_2N_2]M$ Fragments



$[P_2N_2]Ln$ fragments.²¹ The average Ho–C(ring) bond distance is 2.708(2) Å, only slightly shorter than the average Y–C(ring) distances in **3a**.²⁰

Mechanism of C–C Bond Formation. In this study, there is a bifurcation in product formation that is clearly dependent on the central metal ion; for the $[P_2N_2]Y$ and $[P_2N_2]Ho$ fragments, dinuclear coupled diaryl units are formed, while for the $[P_2N_2]Yb$ and $[P_2N_2]Lu$ moieties, only mononuclear products can be isolated. What links these pairs of metal ions is their size: the octahedral Y^{3+} ion has a radius of 1.04 Å, identical to Ho^{3+} due to the well-known lanthanide contraction;³⁴ Yb^{3+} and Lu^{3+} have considerably smaller but similar radii of 1.01 and 1.00 Å, respectively.

Some additional details are worth emphasizing; upon addition of aryllithium solutions in ether to **3a** in toluene at $-78^\circ C$, a white precipitate immediately forms and the solution remains colorless until the ether is evaporated. Once all of the ether is evaporated, then the solution turns dark blue. If performed solely in toluene, the color change occurs without solvent removal, simply upon stirring at room temperature. The fact that no color change is observed before all of the ether is removed in the former method, and the formation of the σ -bonded THF adduct of yttrium(III), **6**, suggests that the first step of the reaction involves formation of an ether-solvated σ -bonded aryl complex, $[P_2N_2]M(\sigma\text{-aryl})(OEt_2)$. The existence of this monophenyl intermediate is supported by isolation of the ether-free Yb derivative, **8**, and by $SiMe_4$ generation in the synthesis of **3a** via σ -bond metathesis of the alkyl complex **2a**. For those larger metal ions, Y^{3+} and Ho^{3+} , the solvated ether is easily removed to generate coordinatively unsaturated intermediates that undergo dimerization to generate dinuclear species with bridging phenyl groups; in the case where ether is not used, direct replacement of the bridging chlorides with bridging aryl groups would generate the same intermediate; this is summarized in Scheme 2.

Bridging alkyl complexes of yttrium(III) are known, for example, $(Cp_2Y)_2(\mu\text{-}Me)_2$, whose solid state structure has been determined and shows a dimer in which the two metal centers are linked together via electron-deficient methyl bridges.^{35,36} Bridging phenyl groups

(32) Fedushkin, I. L.; Bochkarev, M. N.; Schumann, H.; Esser, L.; Kociok-Kohn, G. *J. Organomet. Chem.* **1995**, *489*, 145.

(33) Mashima, K.; Nakamura, A. *J. Chem. Soc., Dalton Trans.* **1999**, 3899.

(34) Shannon, R. D. *Acta Crystallogr. Sect. A* **1976**, *A32*, 751.

(35) Holton, J.; Lappert, M. F.; Ballard, G. H.; Pearce, R.; Atwood, J. L.; Hunter, W. E. *J. Chem. Soc., Dalton Trans.* **1979**, 54.

(36) Holton, J.; Lappert, M. F.; Ballard, G. H.; Pearce, R.; Atwood, J. L.; Hunter, W. E. *J. Chem. Soc., Chem. Commun.* **1976**, 480.

have precedent in the ytterbium complex $\text{Ph}_2(\text{THF})\text{Yb}(\mu\text{-Ph})_3\text{Yb}(\text{THF})_3$.²⁸

In Scheme 2, the bridged intermediate $\{[\text{P}_2\text{N}_2]\text{M}\}_2(\mu\text{-Ar})_2$ then presumably rearranges to give rise to the coupled diaryl moiety sandwiched between two $[\text{P}_2\text{N}_2]\text{M}$ units. This last step is unprecedented and is therefore not easily rationalized. However, it is worth noting that the stability of the trivalent oxidation state of the group 3 elements and the lanthanides is well established, and if one assumes that the bonding in these complexes is largely ionic, then the diaryl coupling does allow a more efficient interaction of the charge of the aryl groups with the $[\text{P}_2\text{N}_2]\text{M}^+$ units.

One further observation deserves mention. During the whole process of metathesis, dimerization, and diaryl coupling, no change in the formal oxidation state of the central metal ion is required. Generally speaking, carbon-carbon bond forming reactions occur via reductive elimination or via migratory insertion. The above sequence involves neither of these well-established processes and thus represents a new kind of C-C bond forming reaction. There is considerable precedent for lanthanide-assisted C-C bond formation via migratory insertion of alkenes or acetylenes into the metal-carbon or metal-hydride bonds.³⁸⁻⁴⁰ The only other example of lanthanide-assisted C-C bond formation that involves neither migratory insertion nor a redox process is the coupling of lanthanide acetylide functionalities to yield dinuclear complexes bridged by C_4R_2 moieties.^{41,42} In these examples, two formally anionic, acetylide ligands couple to form a C-C bond; there is some evidence that suggests that these reactions are also size dependent. Those systems that contain the pentamethylcyclopentadienyl ligand have clearly shown that there is a complicated mixture of steric and electronic factors that lead to product variation in lanthanide-based acetylene oligomerizations and C-C bond formation reactions.^{40,41}

Summary

It has been shown that Y and Ho derivatives of the $[\text{P}_2\text{N}_2]$ macrocyclic ligand are capable of coupling phenyl units via two routes to give sandwiched biphenyl complexes; neither redox nor radical chemistry is involved, and the mechanism is proposed to proceed via a monophenyl species, followed by dimerization and finally C-C bond formation. The monophenyl intermediate is supported by the isolation of $[\text{P}_2\text{N}_2]\text{Yb}(\text{C}_6\text{H}_5)$. The importance of size becomes apparent when viewing results using Lu; it is capable of forming a biphenyl complex via reductive means but is unable to couple Ph units. The availability of coordination sites is clearly significant, as no coupling occurs in more basic solvents such as THF, where monophenyl solvent adducts result. Larger lanthanides such as Sm and La seem to undergo

more complicated processes that are yet to be fully understood.

These coupled diaryl complexes display fluxional behavior that can be rationalized in terms of a rapid migration of the $[\text{P}_2\text{N}_2]\text{M}^+$ fragments over the π -surface of the formally dianionic diaryl bridging unit. This process is analogous to that observed recently in polycyclic aromatic complexes using these same metal ions and ligand systems.²¹

Experimental Section

All manipulations were performed under an atmosphere of dry oxygen-free nitrogen or argon by means of standard Schlenk or glovebox techniques (Vacuum Atmospheres HE-553-2 glovebox equipped with a MO-40-2H purification system and a -40°C freezer). Hexanes and toluene were purchased anhydrous from Aldrich and further dried by passage through a tower of silica and degassed by passage through a tower of Q-5 catalyst under positive pressure of nitrogen.⁴³ Anhydrous diethyl ether was stored over sieves and distilled from sodium benzophenone ketyl under argon. Nitrogen and argon were dried and deoxygenated by passing the gases through a column containing molecular sieves and MnO. Deuterated benzene, toluene, tetrahydrofuran, and cyclohexane were dried by refluxing with molten sodium or potassium metal in a sealed vessel under partial pressure, then trap-to-trap distilled, and freeze-pump-thaw degassed three times. NMR spectra were recorded on either a Bruker AC-200 instrument operating at 200.132 MHz for ^1H spectra, or a Bruker AMX-500 instrument operating at 500.132 MHz for ^1H spectra, or a Bruker AVA-400 instrument operating at 400.132 MHz for ^1H spectra. ^1H NMR spectra were referenced to residual protons in the deuterated solvent and ^{13}C NMR spectra to the ^{13}C atoms therein. $^{31}\text{P}\{^1\text{H}\}$ and ^7Li NMR spectra were referenced to external $P(\text{OMe})_3$ (141.0 ppm with respect to 85% H_3PO_4 at 0.0 ppm) and external LiCl (1.0 M in D_2O). UV-vis spectra were recorded using a Hewlett-Packard 8454 UV-visible spectrophotometer and quartz cuvettes with Teflon Kontes valves. Elemental analyses were performed by Mr. P. Borda of this department. The compounds *syn*- $[\text{P}_2\text{N}_2]\text{Li}_2\cdot\text{C}_4\text{H}_8\text{O}_2$ and $\text{LiCH}_2\text{SiMe}_3$ were prepared according to literature procedures. $\text{YCl}_3\cdot 6\text{H}_2\text{O}$, $\text{LuCl}_3\cdot 6\text{H}_2\text{O}$, $\text{HoCl}_3\cdot 6\text{H}_2\text{O}$, $\text{SmCl}_3\cdot 6\text{H}_2\text{O}$, and $\text{YbCl}_3\cdot 6\text{H}_2\text{O}$ were purchased from Strem and used as received. $\text{YCl}_3(\text{THF})_3$, $\text{LuCl}_3(\text{THF})_3$, $\text{HoCl}_3(\text{THF})_3$, $\text{SmCl}_3(\text{THF})_3$, and $\text{YbCl}_3(\text{THF})_3$ were synthesized according to a literature procedure.⁴⁴ All organic materials were purchased from Aldrich. Phenylbromide, *p*-tolylbromide, and *p*-bromobiphenyl were purified by published procedures.⁴⁵ Phenyllithium, *p*-tolyllithium, and *p*-biphenyllithium were synthesized by dissolving the corresponding aryl bromides in ether and dropwise addition of *n*-BuLi to the reaction mixture. They were isolated as solids or titrated following the literature methods.⁴⁶

Synthesis of $\{[\text{P}_2\text{N}_2]\text{M}\}_2(\mu\text{-Cl})_2$, $\text{M} = \text{Y, Sm, Ho, Yb, Lu, 1a-e}$. To a mixture of *syn*- $[\text{P}_2\text{N}_2]\text{Li}_2\cdot\text{C}_4\text{H}_8\text{O}_2$ (1.90 g, 2.98 mmol) and $\text{MCl}_3(\text{THF})_3$ (2.98 mmol) was added toluene (60 mL). The resulting suspension was stirred at 85°C for 18 h. Filtration through Celite and removal of the solvent in vacuo produced colorless or pale-colored powders. Washing with minimal hexanes allowed isolation of pale yellow **1a** (1.92 g, 98%), pale yellow **1b** (1.91 g, 89%), pale pink **1c** (1.81 g, 83%), yellow **1d** (2.10 g, 95%), and white **1e** (2.17 g, 98%). Crystals could be obtained by slow evaporation of a toluene solution at -40°C .

(37) Cloke, F. G. N. *Chem. Soc. Rev.* **1993**, 17.

(38) Nolan, S. P.; Stern, D.; Marks, T. J. *J. Am. Chem. Soc.* **1989**, *111*, 7844.

(39) Molander, G. A.; Hoberg, J. O. *J. Am. Chem. Soc.* **1992**, *114*, 3123.

(40) Heeres, H. J.; Teuben, J. H. *Organometallics* **1991**, *10*, 1980.

(41) Evans, W. J.; Keyser, R. A.; Ziller, J. W. *Organometallics* **1993**, *12*, 2618.

(42) Forsyth, C. M.; Nolan, S. P.; Stern, C. L.; Marks, T. J.; Rheingold, A. L. *Organometallics* **1993**, *12*, 3618.

(43) Pangborn, A. B.; Giardello, M. A.; Grubbs, R. H.; Rosen, R. K.; Timmers, F. J. *Organometallics* **1996**, *15*, 1518.

(44) Piers, W. E.; Shapiro, P. J.; Bunel, E. E.; Bercaw, J. E. *Synlett* **1990**, 74.

(45) Perrin, D. D.; Armarego, W. L. F. *Purification of Laboratory Chemicals*, 3 ed.; Butterworth-Heinemann Ltd.: Oxford, 1994.

(46) Juaristi, E.; Martinez-Richa, A.; Garcia-Rivera, A.; Cruz-Sanchez, J. S. *J. Org. Chem.* **1983**, *48*, 2603.

1a: ^1H NMR (200 MHz, C_6D_6 , 25 °C) δ 7.90 (m, 4H, *o*-H, phenyl), 6.90 (m, 6H, *m/p*-H, phenyl), 1.43 (AB m's, 4H, ring CH_2), 1.12 (AB m's, 4H, ring CH_2), 0.35 (s, 12H, ring SiMe_2), 0.27 (s, 12H, ring SiMe_2); $^{31}\text{P}\{^1\text{H}\}$ δ -33.8 (d, $J_{\text{YP}} = 84.0$ Hz) Anal. Calcd for $\text{C}_{24}\text{H}_{42}\text{ClYn}_2\text{P}_2\text{Si}_4$: C, 43.86; H, 6.44; N, 4.26. Found: C, 44.24; H, 6.57; N, 4.21.

1b: Anal. Calcd for $\text{C}_{24}\text{H}_{42}\text{ClSmN}_2\text{P}_2\text{Si}_4$: C, 40.11; H, 5.89; N, 3.90. Found: C, 40.67; H, 6.14; N, 3.78.

1c: Anal. Calcd for $\text{C}_{24}\text{H}_{42}\text{ClHoN}_2\text{P}_2\text{Si}_4$: C, 39.31; H, 5.77; N, 3.82. Found: C, 39.62; H, 5.80; N, 3.77.

1d: Anal. Calcd for $\text{C}_{24}\text{H}_{42}\text{ClYbN}_2\text{P}_2\text{Si}_4$: C, 38.88; H, 5.71; N, 3.78. Found: C, 38.98; H, 5.53; N, 3.83.

1e: ^1H NMR (200 MHz, C_6D_6 , 25 °C) δ 7.80 (m, 4H, *o*-H, phenyl), 6.80 (m, 6H, *m/p*-H, phenyl), 1.50 (AB m's, 4H, ring CH_2), 1.10 (AB m's, 4H, ring CH_2), 0.30 (s, 12H, ring SiMe_2), 0.17 (s, 12H, ring SiMe_2); $^{31}\text{P}\{^1\text{H}\}$ δ -26.0 Anal. Calcd for $\text{C}_{24}\text{H}_{42}\text{ClLuN}_2\text{P}_2\text{Si}_4$: C, 38.78; H, 5.69; N, 3.77. Found: C, 38.74; H, 5.67; N, 3.57.

Synthesis of $[\text{P}_2\text{N}_2]\text{M}(\text{CH}_2\text{SiMe}_3)$, $\text{M} = \text{Y, Lu, Ho, and Yb, 2a-d}$. To a slurry of $\{[\text{P}_2\text{N}_2]\text{M}\}_2(\mu\text{-Cl})_2$ (0.48 mmol) in hexanes was added a hexanes solution of $\text{LiCH}_2\text{SiMe}_3$ (0.96 mmol). The resultant cloudy solution was stirred at room temperature for 30 min and filtered through Celite, and the solvent was removed in vacuo to yield **2a** (0.68 g, 97%) as a colorless oil, **2b** (0.74 g, 97%) as a colorless oil that partially solidified on standing, **2c** (0.77 g, 97%) as a white crystalline solid, and **2d** (0.67 g, 87%) as a pale orange solid.

2a: ^1H NMR (200 MHz, C_6D_6 , 25 °C) δ 7.66 (m, 4H, *o*-H, phenyl), 7.10 (m, 6H, *m/p*-H, phenyl), 1.30 (AB m's, 4H, ring CH_2), 1.05 (AB m's, 4H, ring CH_2), 0.48 (s, 9H, alkyl SiMe_3), 0.23 (s, 12H, ring SiMe_2), 0.20 (s, 12H, ring SiMe_2), 0.18 (d, 2H, $J_{\text{YH}} = 2.4$ Hz, Y-CH_2); $^{31}\text{P}\{^1\text{H}\}$ NMR δ -32.1 (d, $J_{\text{YP}} = 81.0$ Hz); ^1H NMR (200 MHz, C_6D_{12} , 25 °C) δ 7.63 (m, 4H, *o*-H, phenyl), 7.28 (m, 6H, *m/p*-H, phenyl), 1.14 (AB m's, 4H, ring CH_2), 1.11 (AB m's, 4H, ring CH_2), 0.19 (s, 9H, alkyl SiMe_3), 0.09 (s, 12H, ring SiMe_2), 0.08 (s, 12H, ring SiMe_2), -0.21 (d, 2H, $J_{\text{YH}} = 2.5$ Hz, Y-CH_2); $^{31}\text{P}\{^1\text{H}\}$ NMR δ -27.8 (d, $J_{\text{YP}} = 83.1$ Hz).

2b: ^1H NMR (200 MHz, C_6D_6 , 25 °C) δ 7.70 (m, 4H, *o*-H), 7.05 (m, 6H, *m/p*-H, phenyl), 1.40 (AB m's, 4H, ring CH_2), 1.05 (AB m's, 4H, ring CH_2), 0.40 (s, 9H, alkyl SiMe_3), 0.30 (s, 2H, Lu-CH_2), 0.23 (s, 12H, ring SiMe_2), 0.20 (s, 12H, ring SiMe_2); $^{31}\text{P}\{^1\text{H}\}$ NMR δ -22.36.

2c: Anal. Calcd for $\text{C}_{28}\text{H}_{53}\text{HoN}_2\text{P}_2\text{Si}_5$: C, 42.84; H, 6.80; N, 3.57. Found: C, 43.50; H, 7.12; N, 3.44.

2d: Anal. Calcd for $\text{C}_{28}\text{H}_{53}\text{N}_2\text{P}_2\text{Si}_5\text{Yb}$: C, 42.40; H, 6.74; N, 3.53. Found: C, 43.07; H, 7.00; N, 3.42.

Synthesis of $\{[\text{P}_2\text{N}_2]\text{M}\}_2\{\mu\text{-}\eta^6\text{-}\eta^6\text{-}(\text{C}_6\text{H}_5)_2\}$, $\text{M} = \text{Y, Ho, 3a,c}$. To a cooled suspension of **1a** or **1c** (0.66 mmol) in toluene (30 mL) was added a toluene suspension of phenyllithium (2.89 mmol, 50 mL) at -78 °C. The mixture was stirred to room temperature and allowed to react for a further 18 h, during which time a pale blue color developed. The reaction mixture was filtered through Celite and the solvent removed in vacuo. The blue residues were extracted into hexanes (25 mL), and cooling to -30 °C yielded **3a** and **3c** as dark blue cubes (0.42 g, 45% and 0.70 g, 69%, respectively).

3a: ^1H NMR (200 MHz, C_7D_8 , 25 °C) δ 7.28 (m, 8H, *o*-H), 7.05 (m, 12H, *m/p*-H, phenyl), 5.10 (dd, 4H, $J_{\text{HH}} = 8.5$ & 6.3 Hz, *m*-H, biphenyl), 4.46 (d, 4H, $J_{\text{HH}} = 8.5$ Hz, *o*-H, biphenyl), 4.18 (t, 2H, $J_{\text{HH}} = 6.0$ Hz, *p*-H, biphenyl), 1.50 (AB m's, 8H, ring CH_2), 1.20 (AB m's, 8H, ring CH_2), 0.50 (s, 24H, ring SiMe_2), 0.20 (s, 24H, ring SiMe_2); $^{31}\text{P}\{^1\text{H}\}$ NMR δ -26.87 (d, $J_{\text{YP}} = 84.1$ Hz) Anal. Calcd for $\text{C}_{60}\text{H}_{94}\text{N}_4\text{P}_4\text{Si}_8\text{Y}_2 \cdot 0.15(\text{toluene})$: C, 52.33; H, 6.82; N, 3.93. Found: C, 52.45; H, 6.90; N, 3.73. UV-vis: $\lambda_{\text{max}} = 615$, $\epsilon_0 = 13\,000$ L mol $^{-1}$ cm $^{-1}$.

3c: Anal. Calcd for $\text{C}_{60}\text{H}_{94}\text{N}_4\text{P}_4\text{Si}_8\text{Ho}_2$: C, 46.50; H, 6.11; N, 3.62. Found: C, 46.40; H, 6.24; N, 3.61. UV-vis: $\lambda_{\text{max}} = 618$, $\epsilon_0 = 14\,000$ L mol $^{-1}$ cm $^{-1}$.

Synthesis of $\{[\text{P}_2\text{N}_2]\text{Y}\}_2\{\mu\text{-}\eta^6\text{-}\eta^6\text{-}\text{C}_6\text{H}_4\text{-p-Me}\}(\text{C}_6\text{H}_4\text{-p-Me})$, **4.** To a mixture of **1a** (0.5 g, 0.38 mmol) and $\text{LiC}_6\text{H}_4\text{-p}$

Me (82 mg, 0.84 mmol) was added a mixture of toluene (10 mL) and Et_2O (5 mL) at room temperature. The colorless mixture was stirred for 30 min, after which the solvents were evaporated, causing a brown/orange color to develop. The brown residues were extracted into toluene (2×5 mL), filtered through Celite, and evaporated to ca. 1 mL. The addition of hexanes (5 mL) and cooling to -30 °C caused **4** to deposit as dark brown prisms (0.17 g, 31%). **4:** ^1H NMR (200 MHz, C_7D_8 , 25 °C) δ 7.05 (m, 8H, *o/p*-H), 6.83 (m, 4H, *m*-H, phenyl), 4.15 (AB m's, 4H, CH), 1.80 (AB m's, 8H, ring CH_2), 1.05 (overlapping m, 7H, ring CH_2 + tolyl- CH_3), 0.70 (s, 12H, ring SiMe_2), 0.04 (s, 12H, ring SiMe_2); $^{31}\text{P}\{^1\text{H}\}$ NMR δ -20.1 (d, $J_{\text{YP}} = 85.5$ Hz); $^{13}\text{C}\{^1\text{H}\}$ NMR (C_7D_8) δ 139.7 (s, phenyl quat. C P_2N_2), 136.8 (s, ipso C, bi-*p*-tolyl), 133.0 (s, ipso C, bi-*p*-tolyl), 130.5 (m, CH P_2N_2 phenyl), 128.6 (m, CH P_2N_2 phenyl), 110.5 (br.s, CH bi-*p*-tolyl), 104.0 (br s, CH bi-*p*-tolyl), 20.3 (s, CH_3 bi-*p*-tolyl), 19.7 (m, CH_2 P_2N_2 ring), 7.60 (s, SiMe_2 ring), 7.10 (s, SiMe_2 ring). Anal. Calcd for $\text{C}_{62}\text{H}_{98}\text{N}_4\text{P}_4\text{Si}_8\text{Y}_2$: C, 52.23; H, 6.93; N, 3.93. Found: C, 51.95; H, 7.13; N, 3.83. UV-vis: $\lambda_{\text{max}} = 465$ ($\epsilon_0 > 10\,000$ L mol $^{-1}$ cm $^{-1}$).

Synthesis of $\{[\text{P}_2\text{N}_2]\text{Y}\}_2\{\mu\text{-}\eta^6\text{-}\eta^6\text{-}(\text{C}_6\text{H}_4\text{-p-Ph})_2\}$, **5.** To a solution of *p*-biphenyllithium in Et_2O (1.9 mL, 0.1 M) was added dropwise a stirred solution of **1a** (0.50 g, 0.38 mmol) in toluene at -78 °C. On warming, a colorless solid was deposited. The mixture was then stirred for 2 h, during which time a slight blue color developed, which intensified upon removal of the solvents in vacuo. The residues were extracted into hexanes (10 mL), filtered through Celite, evaporated to ca. 2 mL, and cooled to -30 °C, yielding **5** as dark blue blocks (0.37 g, 63%). **5:** ^1H NMR (200 MHz, C_6D_6 , 25 °C) δ 7.40 (m, 8H, *o*-H), 7.05 (m, 12H, *m/p*-H, phenyl), 6.50 (m, 4H, bisbiphenyl), 6.40 (m, 4H, bisbiphenyl), 6.20 (m, 2H, *p*-H, bisbiphenyl), 5.80 (m, 4H, bisbiphenyl), 5.50 (m, 4H, bisbiphenyl), 1.20 (AB m's, 8H, ring CH_2), 0.95 (AB m's, 8H, ring CH_2), 0.35 (s, 24H, ring SiMe_2), 0.17 (s, 24H, ring SiMe_2); $^{31}\text{P}\{^1\text{H}\}$ NMR δ -26.87 (d, $J_{\text{YP}} = 84.1$ Hz) Anal. Calcd for $\text{C}_{72}\text{H}_{104}\text{N}_4\text{P}_4\text{Si}_8\text{Y}_2 \cdot (\text{toluene})$: C, 57.71; H, 6.87; N, 3.41. Found: C, 57.97; H, 6.97; N, 3.55. UV-vis: $\lambda_{\text{max}} = 668$, $\epsilon_0 = 7000$ L mol $^{-1}$ cm $^{-1}$.

Synthesis of $[\text{P}_2\text{N}_2]\text{Y}(\text{C}_6\text{H}_4\text{-p-Me})(\text{THF})$, **6.** To a mixture of **1a** (0.30 g, 0.46 mmol) and $\text{LiC}_6\text{H}_4\text{-p-Me}$ (0.25 g, 0.25 mmol) was added a mixture of toluene (10 mL) and THF (5 mL) at room temperature. The colorless mixture was stirred for 30 min, and then the solvents were removed in vacuo. The white residues were extracted into toluene (2×5 mL), filtered through Celite, and evaporated to ca. 1 mL. The addition of hexanes (5 mL) and cooling to -30 °C caused **6** to deposit as white needles (0.15 g, 85%). **6:** ^1H NMR (200 MHz, C_6D_6 , 25 °C) δ 8.15 (m, 4H, tolyl ring), 7.23 (m, 4H, *o*-H), 7.12 (m, 6H, *m/p*-H, phenyl), 3.80 (b, 4H, THF), 2.40 (s, 3H, $\text{C}_6\text{H}_5\text{CH}_3$), 1.40 (AB m's, 4H, ring CH_2), 1.29 (b, 4H, THF), 1.10 (AB m's, 4H, ring CH_2), 0.30 (s, 12H, ring SiMe_2), 0.10 (s, 12H, ring SiMe_2); $^{31}\text{P}\{^1\text{H}\}$ NMR δ -33.90 (d, $J_{\text{YP}} = 56$ Hz) Anal. Calcd for $\text{C}_{35}\text{H}_{57}\text{-Cl}_2\text{N}_2\text{OP}_2\text{Si}_4\text{Y}$: C, 53.55; H, 7.32; N, 3.57. Found: C, 53.27; H, 7.12; N, 3.63.

Synthesis of $[\text{P}_2\text{N}_2]\text{Lu}(\text{C}_6\text{H}_5)\text{-LiCl}$, **7.** To a mixture of **1e** (1.00 g, 0.67 mmol) and PhLi (0.12 g, 1.42 mmol) was added toluene (50 mL) at -78 °C. After stirring for 1 h at this temperature, the mixture was stirred for a further 36 h at room temperature. The solvent was removed in vacuo to afford an off-white oil. Extraction into hexanes (30 mL) and slow evaporation yields **7** as a white microcrystalline solid (0.72 g, 65%). **7:** ^1H NMR (200 MHz, $\text{C}_4\text{D}_8\text{O}$, 25 °C) δ 7.8–6.7 (m, 15H, *PPh/LuPh*), 1.27 (m, 8H, ring CH_2), 0.88 (m, 8H, ring CH_2), 0.35 (s, 3H, SiMe_2), 0.33 (s, 3H, SiMe_2), 0.23 (s, 3H, SiMe_2), 0.20 (s, 3H, SiMe_2), 0.16 (s, 3H, SiMe_2), 0.09 (s, 3H, SiMe_2), 0.06 (s, 3H, SiMe_2), 0.00 (s, 3H, SiMe_2); $^{31}\text{P}\{^1\text{H}\}$ NMR δ -18.7 (s), -20.3 (s); ^7Li NMR δ -0.7 (br, $\nu_{1/2} = 15$ Hz). Anal. Calcd for $\text{C}_{30}\text{H}_{47}\text{N}_2\text{P}_2\text{Si}_4\text{LuLiCl}$: C, 43.55; H, 5.73; N, 3.39. Found: C, 40.19; H, 6.87; N, 3.67.

Synthesis of $\{[\text{P}_2\text{N}_2]\text{Lu}\}_2\{\mu\text{-}\eta^6\text{-}\eta^6\text{-}(\text{C}_6\text{H}_5)_2\}$, **3e.** To a mixture of **1e** (1.15 g, 0.78 mmol), KC_8 (0.21 g, 1.64 mmol), and

biphenyl (0.24 g, 1.60 mmol) was added toluene (60 mL) and Et₂O (20 mL). The mixture was stirred for 48 h and the solvent removed in vacuo. The resulting dark blue mixture was extracted with toluene (50 mL) and filtered through Celite. Slow evaporation of the solvent initially led to the isolation of colorless needles of biphenyl and eventually dark blue prisms of **3e** (0.63 g, 52%). **3e**: ¹H NMR (200 MHz, C₇D₈, 25 °C) δ 7.28 (m, 8H, *o*-H), 7.06 (m, 12H, *m/p*-H, phenyl), 5.04 (br, 4H, *m*-H, biphenyl), 4.41 (d, 4H, *J*_{HH} 8.7 Hz, *o*-H, biphenyl), 4.03 (br, *p*-H, biphenyl), 1.49 (AB m's, 8H, ring CH₂), 1.22 (AB m's, 8H, ring CH₂), 0.54 (s, 24H, ring SiMe₂), 0.20 (s, 24H, ring SiMe₂); ³¹P{¹H} NMR δ -15.4 (s). Anal. Calcd for C₆₀H₉₄N₄P₄Si₈Lu₂: C, 45.90; H, 6.04; N, 3.57. Found: C, 46.20; H, 6.32; N, 3.55. UV-vis: λ_{max} 603, ε₀ 16 000 L mol⁻¹ cm⁻¹.

Synthesis of [P₂N₂]Yb(C₆H₅)₂, **8.** To a mixture of **1d** (1.60 g, 1.08 mmol) and phenyllithium (0.40 g, 4.82 mmol) at -78 °C was added cold toluene (40 mL). The mixture was stirred at room temperature and allowed to react for a further 18 h, during which time a pale green color developed. The reaction mixture was filtered through Celite and the solvent removed in vacuo. The green residues were extracted into hexanes (25 mL), and cooling to -30 °C yielded **8** as orange cubes (0.84 g, 50%) from the green mother liquor. **8**: Anal. Calcd for C₃₀H₄₇N₂P₂Si₄Yb: C, 46.02; H, 6.05; N, 3.58. Found: C, 46.12; H, 6.23; N, 3.64. A green microcrystalline material obtained from the mother liquor was similarly characterized: Anal. Calcd for C₆₀H₉₄N₄P₄Si₈Yb₂: C, 46.02; H, 6.05; N, 3.58. Found: C, 45.95; H, 6.29; N, 3.38.

X-ray Crystallographic Analyses of {[P₂N₂]Y}₂(μ-Cl)₂, **1a, {[P₂N₂]Lu}₂(μ-Cl)₂, **1e**, {[P₂N₂]Ho}₂{μ-η⁶:η⁶-(C₆H₅)₂}, **3c**, {[P₂N₂]Y}₂{μ-η⁶:η⁶-(C₆H₄-*p*-Ph)₂}, **5**, [P₂N₂]Y(C₆H₄-*p*-Me)(THF), **6**, and [P₂N₂]Yb(C₆H₅)₂, **8**.** Crystallographic data were collected on a Rigaku/ADSC CCD diffractometer and appear in Table 1. The final unit cell parameters were obtained by least squares on the setting angles for 20 107 reflections with 2θ = 4.9–64.5°, **1a**, 86 527 reflections with 2θ = 4.0–60.1°, **1e**, 20 751 reflections with 2θ_{max} = 55.8°, **3c**, 12 205 reflections with 2θ = 4.0–63.7°, **5**, 31 264 reflections with 2θ = 4.0–60.2°, **6**, and 35 557 reflections with 2θ_{max} = 55.8°, **8**. The data were

processed⁴⁷ and corrected by Lorentz and polarization effects and absorption (empirical: based on a three-dimensional analysis of a symmetry-equivalent data).

The structures were solved by heavy-atom Patterson methods (**1a**, **5**), Fourier techniques (**1b**), and direct methods (**3c**, **6**, **8**). All non-hydrogen atoms were refined with anisotropic thermal parameters. Hydrogen atoms were fixed in calculated positions with C–H = 0.98 Å and B_H = 1.2_{bonded atom}. Unmodified statistical weights ($w = 1/\sigma^2(F_o)^2$) were employed for all six structures. Neutral atom scattering factors and anomalous dispersion corrections were taken from the *International Tables for X-ray Crystallography*.^{48–50}

Selected bond lengths and bond angles appear in Tables 2–7. Tables of final atomic coordinates and equivalent isotropic thermal parameters, anisotropic thermal parameters, bond lengths and angles, torsion angles, intermolecular contacts, and least-squares planes are included as Supporting Information.

Acknowledgment. We thank NSERC of Canada for generous financial support.

Supporting Information Available: Complete X-ray crystallographic experimental details and tables of final atomic coordinates and equivalent isotropic thermal parameters, anisotropic thermal parameters, bond lengths and angles, torsion angles, intermolecular contacts, and least-squares planes. This material is available free of charge via the Internet at <http://pubs.acs.org>.

OM000755E

(47) *teXsan Crystal Structure Analysis Package*, 1.8 ed.; Molecular Structure Corp.: The Woodlands, TX, 1996.

(48) Cromer, D. T.; Waber, J. T. *International Tables for X-ray Crystallography*; Kynoch Press: Birmingham, U.K., 1974; Vol. IV, p 99.

(49) Creagh, D. C., McAuley, W. J., Wilson, A. J. C., Eds. *International Tables for X-ray Crystallography*; Kluwer Academic Publishers: Boston, MA, 1992; Vol. C, p 200.

(50) Creagh, D. C., McAuley, W. J., Wilson, A. J. C., Eds.; *International Tables for X-ray Crystallography*; Kluwer Academic Publishers: Boston, MA, 1992; Vol. C, p 219.